ARTICLE
Journal of Cellular Biochemistry 110:1504–1511 (2010)

Journal of Cellular Biochemistry

Reciprocal Relationship Between Cytosolic NADH and ENOX2 Inhibition Triggers Sphingolipid-Induced Apoptosis in HeLa Cells

Thomas De Luca,[1] Dorothy M. Morré,[1] and D. James Morré[2]*

[1]*Department of Foods and Nutrition, Purdue University, Stone Hall, 700 W. State Street, West Lafayette, Indiana 47907-2059*

[2]*Department of Medicinal Chemistry and Molecular Pharmacology, Purdue University, 201 S. University Street, West Lafayette, Indiana 47907-2064*

ABSTRACT

ENOX2 (tNOX), a tumor-associated cell surface ubiquinol (NADH) oxidase, functions as an alternative terminal oxidase for plasma membrane electron transport. Ubiquitous in all cancer cell lines studied thus far, ENOX2 expression correlates with the abnormal growth and division associated with the malignant phenotype. ENOX2 has been proposed as the cellular target for various quinone site inhibitors that demonstrate anticancer activity such as the green tea constituent epigallocatechin-3-gallate (EGCg) and the isoflavene phenoxodiol (PXD). Here we present a possible mechanism that explains how these substances result in apoptosis in cancer cells by ENOX2-mediated alterations of cytosolic amounts of NAD^+ and NADH. When ENOX2 is inhibited, plasma membrane electron transport is diminished, and cytosolic NADH accumulates. We show in HeLa cells that NADH levels modulate the activities of two pivotal enzymes of sphingolipid metabolism: sphingosine kinase 1 (SK1) and neutral sphingomyelinase (nSMase). Their respective products sphingosine 1-phosphate (S1P) and ceramide (Cer) are key determinants of cell fate. S1P promotes cell survival and Cer promotes apoptosis. Using plasma membranes isolated from cervical adenocarcinoma (HeLa) cells as well as purified proteins of both bacterial and human origin, we demonstrate that NADH inhibits SK1 and stimulates nSMase, while NAD^+ inhibits nSMase and has no effect on SK1. Additionally, intact HeLa cells treated with ENOX2 inhibitors exhibit an increase in Cer and a decrease in S1P. Treatments that stimulate cytosolic NADH production potentiate the antiproliferative effects of ENOX2 inhibitors while those that attenuate NADH production or stimulate plasma membrane electron transport confer a survival advantage. J. Cell. Biochem. 110: 1504–1511, 2010.

KEY WORDS: APOPTOSIS; ECTO-NOX; NADH OXIDASE; tNOX; CANCER; CAPSAICIN; CERAMIDE; COENZYME Q; (−)-EPIGALLOCATECHIN-3-GALLATE (EGCg); PLASMA MEMBRANE ELECTRON TRANSPORT; SPHINGOMYELINASE (SMase); SPHINGOSINE-1-PHOSPHATE (S1P); SPHINGOSINE KINASE (SK)

Biochemical mechanisms that link growth arrest from antiproliferative chemotherapeutic agents and apoptosis [Radin, 2003], have focused on compounds (e.g., EGCg, capsaicin, cis-platinum, adriamycin, phenoxodiol) that target a cell-surface electron transport activity that catalyzes the reduction of molecular oxygen to water [Morré and Morré, 2003]. Trans-plasma membrane electron transport, accelerated in neoplasms of multiple origins [Larm et al., 1994], oxidizes the reduced pyridine nucleotides (i.e., NADH) generated by this "aerobic glycolysis" [Warburg, 1956; Edinger and Thompson, 2002; Fantin et al., 2006; Wu et al., 2006] to ensure continued glycolytic ATP production. The terminal oxidases for this system, designated ECTO-NOX (ENOX) proteins [Morré and Morré, 2003] are cell-surface hydroquinone oxidases with protein disulfide-thiol interchange activity located at the cell surface that also participate in cell growth. A drug-responsive, cancer-specific variant, ENOX2, serves as the molecular target for quinone site inhibitors with anticancer activity, including epigallocatechin-3-gallate (EGCg) from green tea [Morré et al., 2000] and the anticancer isoflavene phenoxodiol (PXD) [Morré et al., 2007]. These inhibitors induce apoptosis in cancer lines through interactions with the classical Fas death receptor pathway, downstream inactivation of the PI3K/Akt cell survival pathway, cleavage of the X-linked inhibitor of apoptosis (XIAP), activation of the downstream caspase cascade and subsequent cell death [Kamsteeg et al., 2003].

Ceramide, a sphingolipid component of the plasma membrane linked to signaling events preceding growth arrest and apoptotic cell death accumulates [Bose et al., 1995] whereas levels of sphingosine 1-phosphate (S1P), a sphingolipid with the opposing function of

*Correspondence to: D. James Morré, PhD, NOX Technologies, Inc., 1291C Cumberland Avenue, West Lafayette, IN 47906-1075. E-mail: dj_morre@yahoo.com

Received 14 April 2010; Accepted 21 May 2010 • DOI 10.1002/jcb.22724 • © 2010 Wiley-Liss, Inc.
Published online 1 June 2010 in Wiley InterScience (www.interscience.wiley.com).

promoting cell survival, decreases upon treatment with PXD [De Luca et al., 2005]. We have developed a model consistent with the investigations of others whereby ENOX2 inhibitors cause the accumulation of NADH at the inner leaflet of the plasma membrane that would then interact with both neutral sphingomyelinase (nSMase) and sphingosine kinase (SK). This interaction would stimulate nSMase to produce pro-apoptotic ceramide whereas SK would be inhibited to produce less of the pro-survival S1P [Spiegel and Milstien, 2002]. This shift in the sphingolipid "rheostat" to a pro-apoptotic/antiproliferative state, attributes to NADH the novel role of determining cell fate at the signaling microenvironment of the inner plasma membrane surface [Hannun, 1994].

The possibility of direct links between inhibition of the ENOX2 protein by EGCg or PXD, the elevation of ceramide and the pro-apoptotic loss of S1P was indicated from previous work in our laboratory [De Luca et al., 2005]. This study was to extend these findings to a similar response to in vivo levels of NADH modulated experimentally and to different forms of sphingomyelinases. The specific hypothesis to be tested was that the cell surface NADH oxidases of the plasma membrane electron transport system (ECTO-NOX) proteins were directly coupled to the control of ceramide and/or S1P formation through effects on cytosolic levels of NADH and/or NAD^+.

METHODS

Cell lines obtained from the American Type Culture Collection (Rockville, MD) were grown under 5% CO_2 in 175 cm^2 flasks in Minimal Essential Medium (Gibco), pH 7.4, at 37°C with 10% bovine calf serum (heat-inactivated), plus 50 mg/L gentamycin sulfate (Sigma) and harvested by scraping. Cell numbers were determined by counting. Plasma membranes were purified from HeLa cells using aqueous two-phase partitioning as described [Morré and Morré, 1989].

SEPARATION AND QUANTITATION OF LIPIDS BY THIN LAYER CHROMATOGRAPHY AND DENSITOMETRY

For measurements of total sphingolipid content from cell cultures, HeLa cells from 60 or 100 mm tissue culture dishes were harvested by either mechanical scraping or brief incubation with 0.05% trypsin for 10 min at room temperature and transferred to 1.5 mL microcentrifuge tubes. Lipids were extracted by the traditional method of Bligh and Dyer [1959], which involved the addition of 200 μl chloroform/methanol (2:1) and 800 μl water/ethanol (8:1) followed by vigorous mixing for 1 min on a Vortex-Genie 2T at the maximum setting. Organic and aqueous phases were separated by centrifugation at 14,000*g* for 5 min. The organic phase was loaded rapidly and directly using a micropipette onto silica-coated glass plates under a stream of air to expedite evaporation for chromatographic separation.

For ceramide measurements, lipids were resolved using a two-phase solvent system with chloroform–methanol–ammonium hydroxide (100:25:1) as the first solvent and hexane/ethyl ether (65:35) as the second. Using 20 cm long silica gel plates, the first solvent was allowed to migrate 6 cm prior to removal of the plate and drying under compressed air. The second solvent was allowed to migrate 10 cm. Neutral sphingolipids were visualized by spraying the dry chromatograms with 50% sulfuric acid [Walter et al., 1980] followed by heat for a minimum of 15 min at 100°C. Ceramide was identified by comparison with a standard resolved in parallel.

For S1P measurements, lipids were separated using a solvent system of *n*-butanol: ethanol/acetic acid/water (8:2:1:2) and 20 cm long silica gel plates. The solvent was allowed to migrate 10 cm prior to removal of the plate and drying under compressed air. S1P was visualized by spraying the dry chromatograms with either ninhydrin (2 mg/ml in ethanol) or 1.5% ammonium molybdate in 4.2 M phosphoric acid followed by heat for a minimum of 15 min at 100°C.

SK activity assays used exogenous substrate and radiolabeled ATP. Visualization of radiolabeled lipids was by exposing the dry chromatograph to a phosphor screen (Perkin-Elmer) for variable lengths of time (depending on signal and sensitivity) in a sealed exposure cassette at room temperature. The exposed phosphor screen was then processed using a Storage Phosphor Cyclone phosphoimaging system (Perkin-Elmer) at 600 dpi resolution. Visualized spots were quantitated using LabWorks 4.5 densitometry software. Quantitation was relative to a control lane minus test substances.

CELL-FREE ENZYMATIC ASSAYS

For SK, the assay contained in a final volume of 100 μl 50 mM Tris–HCl, pH 7.2, 1 mM EGTA, 10 mM $MgCl_2$, 40 mM octyl-β-D-glucopyranoside, 1 mM ATP including 10 μCi [γ-^{32}P] ATP (Amersham), and 0.5 mM D-erythro-sphingosine (Biomol, Avanti Polar Lipids) [Panka et al., 2001]. Where highly purified recombinant human sphingosine kinase 1 (SK1, ExAlpha) was the source of activity, 0.1–1 μg protein was used (depending on the production lot). Relevant test substances were added in volumes of 2 μl.

For SMase, the reaction mixture contained in a final volume of 100 μl, 50 mM Tris–HCl, pH 7.2, 1 mM EGTA, 10 mM $MgCl_2$, 40 mM octyl-β-D-glucopyranoside and substances to be tested in a 1.5 ml microcentrifuge tube followed by 15 μg sphingomyelin to start the reaction. Reactions were stopped by the addition of organic solvents for lipid extraction.

SPHINGOMYELINASE FROM HUMAN URINE

Proteins from two male human donors were collected by ammonium sulfate precipitation (50–60% of saturation) with centrifugation at 7,710*g* for 15 min. Ammonium sulfate was removed by overnight dialysis at 4°C with stirring.

BODIPY-dUTP/TdT APOPTOSIS ASSAY

BODIPY FL-14-dUTP was from Invitrogen (Cat. No. C7614) and was utilized in an in situ nick translation assay as the labeling agent according to Barrett et al. [2001]. Apoptosis was monitored at 0, 3, 6, 12, and 24 h of inhibitor treatment. The number of fluorescent cells reached a maximum at about 6 h in both HeLa and MCF-10A cells and plateaued thereafter.

GROWTH MEASUREMENTS

Cell growth (cell survival) was determined using a 96-well plate assay. Cells were fixed by glutaraldehyde and stained with 1% aqueous crystal violet. Absorbance was determined at 580 nm with an automated plate reader.

RESULTS

ENOX2 INHIBITORS SLOW THE GROWTH OF HeLa CELLS AND INDUCE APOPTOSIS IN CANCER BUT NOT IN NON-CANCER CELLS

Here we demonstrate that the two inhibitors under investigation, EGCg and PXD, known to specifically target ENOX2 at low doses not effecting other targets, slow the growth of HeLa (human cervical carcinoma) cells and induce apoptosis without similar effects on non-cancer MCF-10A (human mammary epithelia) cells (Table I; see Discussion Section for additional examples). Cells of non-cancerous human cervical tissue also were examined and shown to lack ENOX2. Cell numbers for HeLa cells reached an IC_{50} concentration at 0.2 and 2 μM for BT-20 (human mammary adenocarcinoma) cell lines, respectively, for PXD and 0.003 and 0.01 μM for EGCg. The immediate response of the cancer lines to PXD or EGCg was a rapid cessation of cell enlargement with the ultimate result of creating a population of small cells unable to divide further, which subsequently underwent apoptosis (Fig. 1A). With times as short as 6 h, incubation with 10 μM PXD or 100 μM EGCg, apoptosis was seen in HeLa cells using the BODIPY-dUTP/TdT assay (Fig. 1A). A similar apoptotic response to EGCg was previously reported for HeLa cells using DAPI stain [Morré et al., 2000]. With the non-cancer MCF-10A cells, neither PXD nor EGCg resulted in apoptosis in parallel to the lack of effect of PXD on growth and ENOX activity in non-cancer cells. For non-cancer MCF-10A cells, the IC_{50} concentration exceeded 20 μM.

ENOX INHIBITORS INCREASE CYTOSOLIC NADH LEVELS

A major premise of the work reported here is that apoptosis is initiated by changes in cytosolic NADH resulting from ENOX2 inhibition. Relative increases in NADH estimated in HeLa cells from fluorescence measurements averaged over 30 min of inhibitor addition were 100 ± 36 pmol/10^6 cells for 50 μM EGCg and 125 ± 34 pmol/10^6 cells for 1 μM PXD representing increases of 35% and 44%, respectively. Addition of 100 μM ferricyanide or 100 μM pyruvate reduced the NADH levels by 182 and 113 pmol/10^6 cells, respectively, to very nearly the levels observed in the absence of inhibitor and completely blocked the ability of either 50 μM EGCg or 1 μM PXD to induce apoptosis.

TABLE I. Dose–Response of Growth and ENOX2 Activity of Cell Lines to Phenoxodiol (PXD) and EGCg

	IC_{50} μM			
	Growth		ENOX2 activity[a]	
Cell line	PXD	EGCg	PXD	EGCg
HeLa	0.2	8	0.2	0.003
BT-20	2	8	2	0.01
MCF-10A	>20	>80	Not inhibited	Not inhibited

[a]ENOX activity was measured spectrophotometrically from the rate of oxidation of NADH, an impermeant substrate, based on the decrease in A_{340}. ENOX activity of MCF-10A cells which lack ENOX2 was not inhibited by either phenoxodiol (PXD) or EGCg.

HeLa cells contain 150 pmol NADH/mg protein and 55 pmol NAD^+/mg protein to give a ratio of NADH/NAD^+ of 2.7. Assuming ca. 300 pg protein/cell, 10^6 cells would contain 45 pmol NADH approximating levels determined by NADH fluorescence. Assuming a spherical cell 5 μm in diameter, the NADH concentration in the cytosol would be 5 μM. A 10-fold increase at the cytosolic surface of the plasma membrane plus a corresponding more than doubling of the NADH/NAD^+ ratio should be sufficient to bring the presumed in vivo and the demonstrated in vitro responses to pyridine nucleotide levels into alignment for the HeLa cell experimental system.

As demonstrated above, inhibition of ENOX2 activity in cancer cells and the attendant block of plasma membrane electron transport did result in the accumulation of NADH at the cytosol/plasma membrane interface of the affected cells (Fig. 1B). With both PXD and EGCg, NADH fluorescence at the borders of HeLa cells was observed by microscopy to be markedly increased in the inhibited cells as a means of demonstrating that cytosolic levels of NADH increased as the result of inhibition of the activity of ENOX2 by both PXD and EGCg.

INCREASED NADH RESULTING FROM ENOX2 CELL SURFACE INHIBITION INHIBITS PLASMA MEMBRANE-ASSOCIATED SPHINGOSINE KINASE (SK) AND LOWERS LEVELS OF PRO-SURVIVAL SPHINGOSINE-1-PHOSPHATE (S1P)

Here experiments were carried out to determine the possible response of plasma membrane-associated SK and levels of pro-survival S1P assayed in situ and in cell free systems to pyridine nucleotide levels. Following a transient stimulation with PXD at 3 h, S1P decreased as a function of time for HeLa cells treated with either 10 μM PXD or 10 μM EGCg between 3 and 24 h compared to vehicle alone. After 24 h, the radiolabeled S1P content was reduced by about 60% with EGCg and by nearly 90% by PXD, both of which are potent ENOX2 inhibitors (approximately 100% inhibition of ENOX2 at the concentrations tested) (Fig. 1C).

SK activity was decreased in response to 1.5 mM NADH (Fig. 2A). Both NADH and coenzyme Q_{10} (CoQ_{10}) inhibited SK activity for isolated HeLa cell plasma membranes. NAD^+ at the same concentration of 1.5 mM was without effect (not shown).

From the dose–response of SK of HeLa cell plasma membranes to NADH, the EC_{50} for inhibition was estimated to be about 600 μM (Fig. 2B,C). Capsaicin added to block NADH oxidation by endogenous ENOX2 was without effect when added alone but enhanced inhibition slightly when combined with 1.5 mM NADH (Fig. 2B). NADH consistently inhibited recombinant SK as well (Fig. 2C), whereas NAD^+ had no effect (Fig. 2D). Addition of 1.5 mM or 150 μM NAD^+ to 1.5 mM or 150 μM NADH did not affect inhibition of HeLa plasma membrane SK (not shown) suggesting that it was the absolute level of NADH that was inhibitory rather than the ratio of NADH to NAD^+.

Plasma membranes of mammalian cells are normally impermeable to pyridine nucleotides. Therefore, HeLa cells were treated with low concentrations of the detergent saponin in order to create small

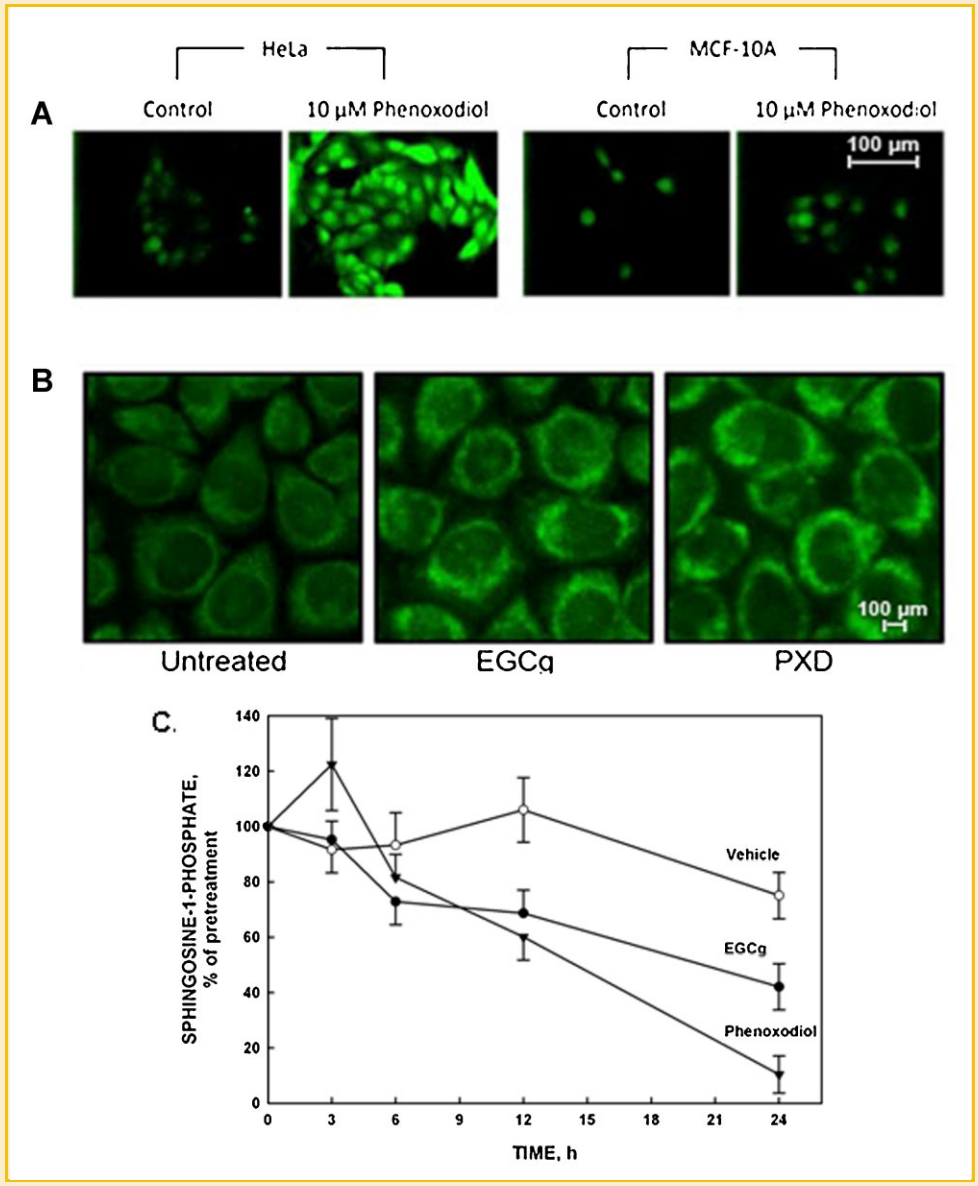

Fig. 1. HeLa cell response to ENOX2 inhibitors. A: BODIPY-dUPT/TdT assay for apoptosis in HeLa and MCF-10A cells after 6 h incubation with 10 μM phenoxodiol. Scale = 100 μM. B: Increased intracellular fluorescence from NADH in HeLa cells following 30 min incubation with 10 μM EGCg or 10 μM phenoxodiol (PXD) for 30 min. Excitation wavelength: 340 nm. Emission wavelength: 460 nm. Scale = 100 μm. C: Sphingosine-1-phosphate content (radiolabeled) in HeLa cells treated with vehicle (DMSO) alone or 10 μM phenoxodiol or EGCg dissolved in DMSO. Sphingosine-1-phosphate was visualized on resolved silica gel plates by spraying with sodium molybdate in phosphoric acid. Results were standardized to untreated control samples.

pores in the membrane. When exogenous NAD^+ or NADH was added, only NADH inhibited the production of S1P whereas NAD^+ did not inhibit (Fig. 2E). NADH also inhibited the SK activity of plasma membranes from soybean (*Glycine max*) (not shown).

In vivo elevation of NADH levels through transient transfection (efficiency of ca. 60%) of HeLa cells with aldehyde dehydrogenase followed by treatment with acetaldehyde (10 μM–10 mM) exhibited a log linear relationship between total S1P formation and expected levels of NADH generated (not shown). S1P levels of mock-transfected or non-transfected HeLa cells not overexpressing aldehyde dehydrogenase did not respond to increasing concentrations of acetaldehyde.

SPHINGOMYELINASE (SMASE)

A reciprocal relationship of SMase was investigated in parallel to that of SK leading to accumulation of pro-apoptotic levels of ceramide. In contrast to SK which was inhibited by NADH, SMase activity was stimulated by NADH (Fig. 3A). This was not due to generation of a reducing environment as GSH (1 mM) inhibited whereas CoQ_{10} was largely without effect (Table II).

The dose–response of activation of bacterial neutral SMase yielded an approximate 50% stimulation at 1 mM NADH whereas 1 mM NAD^+ resulted in an almost 60% inhibition (Fig. 3A). A SMase from urine also demonstrated similar responses to 150 μM NADH

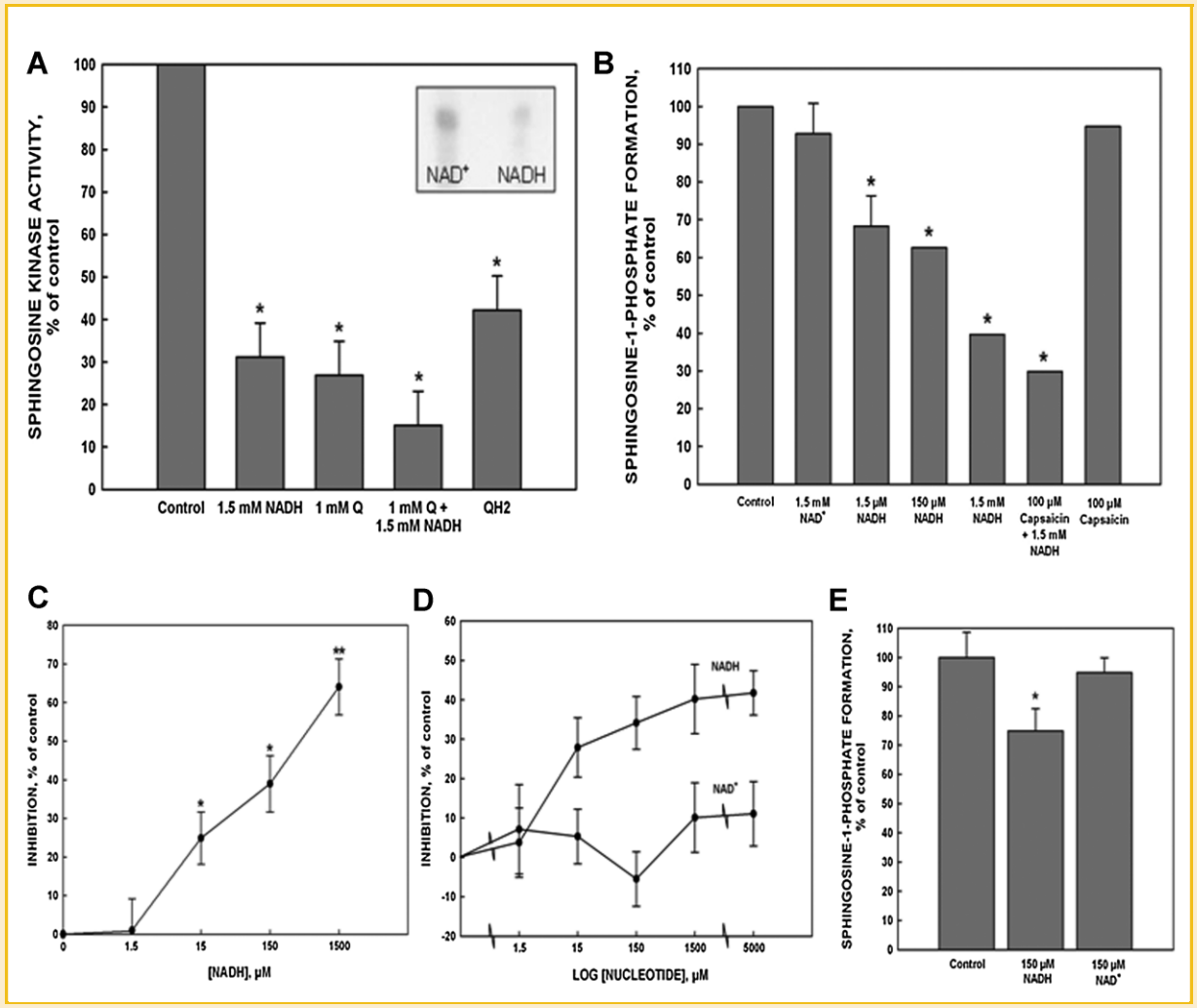

Fig. 2. Response of SK based on sphingosine-1-phosphate (SIP) formation to oxidized or reduced coenzyme Q (A) and inhibition by NADH but not NAD^+ (B–E). A: S1P formation by HeLa cell plasma membranes and inhibition by NADH, coenzyme Q10 (Q) and reduced coenzyme Q10 (QH2). γ32-ATP donated radioactive phosphate to sphingosine in the kinase reaction. Results were standardized to untreated control samples. Inset: Thin layer chromatography confirming inhibition of S1P formation by NADH (1.5 mM). B: Response of S1P formation by HeLa cell plasma membranes to increasing amounts of NADH with an IC50 of about 150 μM ($P < 0.01$). NADH alone and 1.5 mM NADH + 100 μM capsaicin were different from the control value ($P < 0.001$) but not from each other. Bars without standard deviations were not repeated. C: HeLa cell plasma membrane where NADH inhibited with an IC50 of about 150 μM ($P < 0.01$). D: As in (B) with 0.1 μg/assay of recombinant human SK 1. NAD^+ did not inhibit. E: As in (B) with HeLa cells permeabilized by treatment with low concentrations of the detergent saponin in order to create pores in the membrane. NADH but not NAD^+ inhibited the production of S1P.

(Fig. 3B). We observed a log linear increase in bacterial SMase activity up to 1.5 mM NADH (Fig. 3C).

DISCUSSION

ENOX2 inhibitors are well-established inducers of apoptosis in cancer but not in non-cancer cells. Examples include EGCg [Ahmad et al., 1997; Chen et al., 1998; Katdare et al., 1998; Pascha et al., 1998; Morré et al., 2000], PXD [Kamsteeg et al., 2003; Kelly and Husband, 2003; Alvero et al., 2006], and capsaicin [Morré et al., 1995; Ito et al., 2004; Kim et al., 2004; Lee et al., 2004; Chow et al., 2007; Sánchez et al., 2007] encompassing a broad spectrum of human ovarian [Kamsteeg et al., 2003; Alvero et al., 2006], leukemic [Kelly and Husband, 2003; Ito et al., 2004], prostate [Pascha et al., 1998; Kelly and Husband, 2003; Mori et al., 2006; Sánchez et al., 2007], colon [Kelly and Husband, 2003; Kim et al., 2004, 2007], hepatoma [Lee et al., 2004; Baek et al., 2008], breast [Katdare et al., 1998; Morré et al., 1995, 2000; Tuoya et al., 2006], cervical [Morré et al., 1995, 2000], lung [Kelly and Husband, 2003], and gastric [Kelly and Husband, 2003; Chow et al., 2007; Wang et al., 2009] cancer cell lines.

Antisense experiments were carried out with HeLa cells by Tang et al. [2008]. The results showed that antisense specific for the ENOX2 splice variant eliminated growth inhibition by EGCg. Similarly the phenotype of depleted ENOX2 expression by RNA interference eliminated the cell growth response to EGCg [Liu et al., 2008]. Similarly response to EGCg and PXD not seen in wild-type

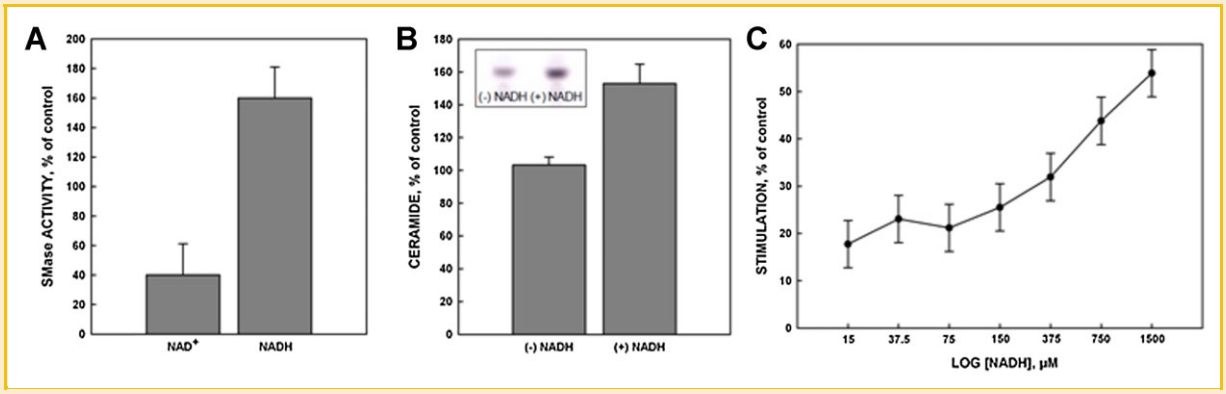

Fig. 3. Stimulation of sphingomyelinase by NADH but not NAD^+. Averages of three determinations ± standard deviations. A: Neutral sphingomyelinase from *S. aureus* (4 mU, Sigma S-8633). Values for 1 mM NAD^+ or NADH over 45 min of incubation were significantly different from the control values ($P < 0.05$). B: Neutral sphingomyelinase (50 μg total protein) isolated from human urine stimulated by 1.5 mM NADH. Inset: Representative chromatogram. C: Bacterial sphingomyelinase.

cells was observed in mouse embryo fibroblasts from ENOX2-overexpressing transgenic mice [Yagiz et al., 2007].

Combination of EGCg or PXD with 100 μM ferricyanide to stimulate plasma membrane electron transport in HeLa cells and lower NADH levels back to normal eliminated the growth inhibition due to both PXD and EGCg and completely prevented PXD- or EGCg-induced apoptosis [L.-Y. Wu et al., unpublished results].

Based on kinetics, the rapid increase at about 30 min followed by a gradual slowing most likely represents ceramide formation by the SMase pathway rather than by de novo synthesis [De Luca et al., 2005]. In situ generation of ceramide from de novo synthesis using [^{3}H] sphingosine showed that biosynthetic elevation of ceramide occurred at 4 h, much slower than in the sphingomyelin pathway, and reached a plateau at 8 h [Bose et al., 1995].

Products of plasma membrane redox expected to result from inhibition of ENOX2 include a change in the ratio of oxidized to reduced coenzyme Q_{10} of the plasma membrane and an increase in reduced pyridine nucleotides. Both neutral and acidic SMase were activated by NADH and inhibited by NAD^+. Thus, they would be expected to contain adenine nucleotide binding motifs within their primary amino acid sequence. The typical adenine nucleotide-binding motif (GXGXXG) with downstream remote acidic residues D or E is represented in human nSMase (human sphingomyelin phosphodiesterase 2) by the sequence G347XGXGXXA(E353) absent from bacterial sphingomyelinase. G102XAXXS (E113) in the bacterial sequence aligns approximately with a G79XGXXV(E92) in the human sequence.

TABLE II. Response of Neutral Sphingomyelinase From *S. aureus*

Addition	Ceramide, % of control
NADH 1 mM	160 ± 20
NAD^+ 1 mM	60 ± 20
GSH 1 mM	8 ± 2
GSSG 1 mM	16 ± 4
H_2O_2 0.3%	30 ± 6
Coenzyme Q_{10} 1 mM	60 ± 6
Coenzyme $Q_{10}H_2$ 1 μM	45 ± 6

Both of the two ENOX2 inhibitors investigated, PXD and EGCg, are potent inducers of apoptosis [Kamsteeg et al., 2003]. A possible mechanism by which Akt functions as a promoter of survival is through the induction of c-FLIP expression and blocking the extrinsic apoptotic pathway [Panka et al., 2001; Suhara et al., 2001]. In epithelial ovarian cancer cells, PXD induces caspase-dependent apoptotic processes involving both extrinsic (death receptor) and intrinsic (mitochondrial) pathways [Alvero et al., 2008]. Indications are that XIAP degradation occurs faster than Akt degradation and that phospho-Akt degradation may occur faster than Akt degradation.

PXD inhibits Akt phosphorylation and induces its degradation [Alvero et al., 2006, 2008]. Accompanying the decrease in XIAP from reduced phosphorylation of Akt along with a decrease in total Akt between 8 and 16 h is the appearance of the p30 XIAP fragment at 16 and 24 h from cleavage by activated caspase −3, −8, and −9 [Alvero et al., 2006]. Alternatively, Akt activation can be regulated by ceramide via a ceramide-activated protein phosphatase 2 (PP2A) or by the downstream metabolite of ceramide, S1P [Igarashi et al., 2001; Pettus et al., 2002]. Dysfunctional metabolism of the second messenger ceramide in cancer cells contributes to the multi-drug resistance phenotype of some cancers. Drug-induced ceramide accumulation inhibits proliferation, induces apoptosis and promotes differentiation [Geilen et al., 1997]. The results with okadaic acid [De Luca et al., 2009] support the concept that ceramide might block activation of Akt by inhibiting its translocation to the cell membrane [Stratford et al., 2001] rather than by promoting its dephosphorylation by phosphatases. Furthermore, an increase in long-chain C16-ceramide, the most abundant species produced by SMase activation at the plasma membrane may contribute to the degradation of XIAP and FLIP by activating the proteosome [Kroesen et al., 2003]. By whatever mechanism, the degradation of XIAP has been suggested to be responsible both for PXD-induced apoptosis [Alvero et al., 2006, 2008] and for the resensitization of resistant melanoma cells to carboplatin [Kluger et al., 2007].

The link between ceramide overproduction by the plasma membrane and G_1 arrest is the reciprocal relationship where SMase is stimulated. Whereas the SK-catalyzed formation of S1P is

inhibited by both the $Q_{10}H_2$ and NADH products of plasma membrane electron transport, SMase is activated by $Q_{10}H_2$ and NADH. Human SK1 contains at least two putative adenine nucleotide binding motifs, S299XGXXG (D320) and G419XGXXA (E428), following the pattern of GXGXXG together with a downstream remote acidic D or E.

If NADH at the cytosolic surface of the plasma membrane is pro-apoptotic by enhancing ceramide and lowering S1P, it follows that acceleration of cytosolic NADH production also might be pro-apoptotic. In this regard, additions of acetaldehyde to HeLa cells overexpressing aldehyde dehydrogenase stimulated SMase and inhibited SK in a dose-dependent manner.

Our findings show not only responses to products of inhibition of ENOX2 and cell enlargement in cancer cells but a reciprocal relationship between effects of these products to activate SMase to increase ceramide as observed with contact inhibition of cell growth and growth inhibition in general [Hannun, 1994]. SK, the enzyme that phosphorylates sphingosine to form S1P, in contrast, is inhibited. S1P is a critical pro-growth, antiapoptotic messenger regulator [Spiegel and Milstien, 2002], the levels of which may be determined by either relative ratios of NADH and NAD^+ or the absolute amounts of NADH or both. An involvement of the "sphingolipid rheostat" in determining cell fate is evident in the work in many laboratories with a variety of cell types and experimental modulators [Maceyka et al., 2002] and its regulation by pyridine nucleotides adds to its importance.

REFERENCES

Ahmad N, Feyes DK, Nieminen AL, Agarwal R, Mukhtar H. 1997. Green tea constituent epigallocatechin-3-gallate and induction of apoptosis and cell cycle arrest in human carcinoma cells. J Natl Cancer Inst 89:1881–1886.

Alvero AB, O'Malley D, Brown D, Kelly G, Garg M, Chen W, Rutherford T, Mor G. 2006. Molecular mechanism of phenoxodiol-induced apoptosis in ovarian carcinoma cells. Cancer 106:599–608.

Alvero AB, Kelly M, Rossi P, Leiser A, Brown D, Rutherford T, Mor G. 2008. Anti-tumor activity of phenoxodiol: From bench to clinic. Future Oncol 4:475–482.

Baek YM, Hwang HJ, Kim SW, Hwang HS, Lee SH, Kim JA, Yun JW. 2008. A comparative proteomic analysis for capsaicin-induced apoptosis between human hepatocarcinoma (HepG2) and human neuroblastoma (SK-N-SH) cells. Proteomics 8:4748–4767.

Barrett KL, Willingham JM, Garvin AJ, Willingham MC. 2001. Advances in cytochemical methods for detection of apoptosis. J Histochem Cytochem 49:821–832.

Bligh EG, Dyer WJ. 1959. A rapid method of total lipid extraction and purification. Can J Biochem Physiol 37:911–917.

Bose R, Verheij M, Haimovitz-Friedman A, Scotto K, Fuks Z, Kolesnick R. 1995. Ceramide synthase mediates daunorubicin-induced apoptosis: An alternative mechanism for generating death signals. Cell 82:405–414.

Chen ZP, Schell JB, Ho CT, Chen KY. 1998. Green tea epigallocatechin gallate shows a pronounced growth inhibitory effect on cancerous cells but not on their normal counterparts. Cancer Lett 129:173–179.

Chow J, Norng M, Chang J, Chai J. 2007. TRPV6 mediates capsaicin-induced apoptosis in gastric cancer cells-mechanisms behind a possible new "hot" cancer treatment. Biochim Biophys Acta 1773:565–576.

De Luca T, Morré DM, Zhao H, Morré DJ. 2005. NAD^+/NADH and/or CoQ/$CoQH_2$ ratios from plasma membrane electron transport may determine ceramide and sphingosine-1-phosphate levels accompanying G1 arrest and apoptosis. BioFactors 25:43–60.

De Luca T, Bosneaga E, Morré DM, Morré DJ. 2009. Downstream targets of altered sphingolipid metabolism in response to inhibition of ENOX2 by phenoxodiol. BioFactors 34:253–260.

Edinger AL, Thompson CB. 2002. Antigen-presenting cells control T cell proliferation by regulating amino acid availability. Proc Natl Acad Sci USA 99:1107–1110.

Fantin VR, St-Pierre J, Leder P. 2006. Attenuation of LDH-A expression uncovers a link between glycolysis, mitochondrial physiology, and tumor maintenance. Cancer Cell 9:425–434.

Geilen CC, Wieder T, Orfanos CE. 1997. Ceramide signalling: Regulatory role in cell proliferation, differentiation and apoptosis in human epidermis. Arch Dermatol Res 289:559–566.

Hannun YA. 1994. The sphingomyelin cycle and the second messenger function of ceramide. J Biol Chem 269:3125–3128.

Igarashi J, Bernier SG, Michel T. 2001. Sphingosine 1-phosphate and activation of endothelial nitric-oxide synthase. Differential regulation of Akt and MAP kinase pathways by EDG and bradykinin receptors in vascular endothelial cells. J Biol Chem 276:12420–12426.

Ito K, Nakazato T, Yamato K, Miyakawa Y, Yamada T, Hozumi N, Segawa K, Ikeda Y, Kizaki M. 2004. Induction of apoptosis in leukemic cells by homovanillic acid derivative, capsaicin, through oxidative stress: Implication of phosphorylation of p53 at Ser-15 residue by reactive oxygen species. Cancer Res 64:1071–1078.

Kamsteeg M, Rutherford T, Sapi E, Hanczaruk B, Shahabi S, Flick M, Brown D, Mor G. 2003. Phenoxodiol—an isoflavone analog—induces apoptosis in chemoresistant ovarian cancer cells. Oncogene 22:2611–2620.

Katdare M, Osborne MP, Telang NT. 1998. Inhibition of aberrant proliferation and induction of apoptosis in pre-neoplastic human mammary epithelial cells by natural phytochemicals. Oncol Rep 5:311–315.

Kelly GE, Husband AJ. 2003. Flavonoid compounds in the prevention and treatment of prostate cancer. Methods Mol Med 81:377–394.

Kim CS, Park WH, Park JY, Kang JH, Kim MO, Kawada T, Yoo H, Han IS, Yu R. 2004. Capsaicin, a spicy component of hot pepper, induces apoptosis by activation of the peroxisome proliferators-activated receptor gamma in HT-29 human colon cancer cells. J Med Food 7:267–273.

Kim YM, Hwang JT, Kwak DW, Lee YK, Park OJ. 2007. Involvement of AMPK signaling cascade in capsaicin-induced apoptosis of HT-29 colon cancer cells. Ann N Y Acad Sci 1095:496–503.

Kluger HM, McCarthy MM, Alvero AB, Sznol M, Ariyan S, Camp RL, Rimm RL, Mor G. 2007. The X-linked inhibitor of apoptosis protein (XIAP) is up-regulated in metastatic melanoma, and XIAP cleavage by phenoxodiol is associated with carboplatin sensitization. J Transl Med 5:6.

Kroesen BJ, Jacobs S, Pettus BJ, Sietsma H, Kok JW, Hannun YA, de Leij LF. 2003. BcR-induced apoptosis involves differential regulation of C16 and C24-ceramide formation and sphingolipid-dependent activation of the proteasome. J Biol Chem 278:14723–14731.

Larm JA, Vaillant F, Linnane AW, Lawen A. 1994. Up-regulation of the plasma membrane oxidoreductase as a prerequisite for the viability of human Namalwa rho 0 cells. J Biol Chem 269:30097–30100.

Lee YS, Kang YS, Lee JS, Nicolova S, Kim JA. 2004. Involvement of NADPH oxidase-mediated generation of reactive oxygen species in the apoptotic cell death by capsaicin in HepG2 human hepatoma cells. Free Radic Res 38:405–412.

Liu SC, Yang JJ, Shao KN, Chueh PJ. 2008. RNA interference targeting tNOX attenuates cell migration via a mechanism that involved membrane association of Rac. Biochem Biophys Res Commun 365:672–677.

Maceyka M, Payne SG, Milstien S, Spiegel S. 2002. SK, sphingosine-1-phosphate, and apoptosis. Biochim Biophys Acta 1585:193–201.

Mori A, Lehmann S, O'Kelly J, Kumagai T, Desmond JC, Pervan M, McBride WH, Kizaki M, Koeffler HP. 2006. Capsaicin, a component of red peppers, inhibits the growth of androgen-independent, p53 mutant prostate cancer cells. Cancer Res 66:3222–3229.

Morré DJ, Morré DM. 1989. Preparation of mammalian plasma membranes by aqueous two-phase partition. Biotechniques 7:946–948, 956–958.

Morré DJ, Morré DM. 2003. Cell surface NADH oxidases (ECTO-NOX proteins) with roles in cancer, cellular time-keeping, growth, aging and neurodegenerative diseases. Free Radic Res 37:795–808.

Morré DJ, Chueh PJ, Morré DM. 1995. Capsaicin inhibits preferentially the NAHD oxidase and growth of transformed cells in culture. Proc Natl Acad Sci USA 92:1831–1835.

Morré DJ, Bridge A, Wu LY, Morré DM. 2000. Preferential inhibition by (−)-epigallocatechin-3-gallate of the cell surface NADH oxidase and growth of transformed cells in culture. Biochem Pharm 60:937–946.

Morré DJ, Chueh PJ, Yagiz K, Balicki A, Kim C, Morré DM. 2007. ECTO-NOX target for the anticancer isoflavene phenoxodiol. Oncology Res 16:299–312.

Panka DJ, Mano T, Suhara T, Walsh K, Mier JW. 2001. Phosphatidylinositol 3-kinase/Akt activity regulates c-FLIP expression in tumor cells. J Biol Chem 276:6893–6896.

Pascha AG, Butler R, Young CY. 1998. Induction of apoptosis in prostate cancer cell lines by the green tea component, (−)-epigallocatechin-3-gallate. Cancer Lett 120:1–7.

Pettus BJ, Chalfant CE, Hannun YA. 2002. Ceramide in apoptosis: An overview and current perspectives. Biochim Biophys Acta 1585:114–125.

Radin NS. 2003. Killing tumours by ceramide-induced apoptosis: A critique of available drugs. Biochem J 371:243–256.

Sánchez AM, Malagarie-Cazenave S, Olea N, Vara D, Chiloeches A, Díaz-Laviada I. 2007. Apoptosis induced by capsaicin in prostate PC-3 cells involves ceramide accumulation, neutral sphingomyelinase, and JNK activation. Apoptosis 12:2013–2024.

Spiegel S, Milstien S. 2002. Sphingosine 1-phosphate, a key cell signaling molecule. J Biol Chem 277:25851–25854.

Stratford S, DeWald DB, Summers SA. 2001. Ceramide dissociates 3′-phosphoinositide production from pleckstrin homology domain translocation. Biochem J 354:359–368.

Suhara T, Mano T, Oliveira BE, Walsh K. 2001. Phosphatidylinositol 3-kinase/Akt signaling controls endothelial cell sensitivity to Fas-mediated apoptosis via regulation of FLICE-inhibitory protein (FLIP). Circ Res 89:13–19.

Tang X, Morré DJ, Morré DM. 2008. Antisense experiments demonstrate an exon 4 minus splice variant mRNA as the basis for expression of tNOX, a cancer-specific cell surface protein. Oncol Res 16:557–567.

Tuoya , Baba N, Shimoishi Y, Murata Y, Tada M, Koseki M, Takahat K. 2006. Apoptosis induction by dohevanil, a DHA substitutive analog of capsaicin, in MCF-7 cells. Life Sci 78:1515–1519.

Walter VP, Kloppel IG, Deimling IG, Morré DJ. 1980. Alterations in neutral glycosphingolipids from transplantable hepatomas and in sera of rats bearing transplantable hepatomas. Can Biochem Biophys 4:145–151.

Wang H-M, Chueh P-J, Chang S-P, Yang C-L, Shao K-N. 2009. Effect of capsaicin on tNOX (ENOX2) protein expression in stomach cancer cells. BioFactors 34:209–217.

Warburg O. 1956. On the origin of cancer cells. Science 123:309–314.

Wu M, Neilson A, Swift AL, Moran R, Tamagnine J, Parskow D, Armistead S, Lemire K, Orrel J, Teich J, Chomicz S, Ferrick DA. 2006. Multiparameter metabolic analysis reveals a close link between attenuated mitochondrial bioenergetic function and enhanced glycolysis dependency in human tumor cells. Physiol Cell Physiol 292:C125–C136.

Yagiz K, Wu L-Y, Kuntz CP, Morré DJ, Morré DM. 2007. Mouse embryonic fibroblast cells from transgenic mice overexpressing tNOX exhibit an altered growth and drug response phenotype. J Cell Biochem 101:295–306.